The greater ease of rotation about the exocyclic C–C bond in triplet phenylcarbene implies that a reactive conformation can be achieved more readily than in the case of the singlet, which is in agreement with the observed relative intramolecular reactivities. Moreover, reaction of the triplet might take place with no rotation about the bond to the carbenic carbon. The minimum energy planar conformation also has an odd electron in the plane of the ring, suitably oriented for reaction with a neighboring double bond. In order to attempt to determine the relative ease of the two modes of attack between the two cases, we performed model HF/STO-3G and HF/3-21G calculations of the attack of triplet methylene on ethene.[24-26] In these calculations two modes of approach were considered (parts a and b of Figure 1). In the first case, the methylene p orbital is attacking the double bond, whereas the second type of approach involves attack by the σ orbital, which lies in the methylene plane. The C$\cdots$C forming bond was fixed at a distance of 2.0 Å, typical for C–C partially formed bonds in transition structures. All other parameters were optimized with a C_s symmetry constraint in both cases. Both sets of calculations suggest that attack by the in-plane orbital, as in Figure 1b, is significantly preferred (by 16.7 kcal/mol at the HF/STO-3G level and by 21.6 kcal/mol at the HF/3-21G level). The related structure, Figure 1c, is only 0.3 kcal/mol higher in energy. Thus, the minimum energy conformation of **5** has the exocyclic CH group already suitably oriented for intramolecular insertion in the double bond. This model is obviously somewhat crude, but the qualitative conclusions should persist even if a higher level of theory were employed. The geometry of approach implied in Figure 1b resembles the transition structure, which Fueno and co-workers found from ab initio molecular orbital calculations (MRDCI/4-31G**//HF/4-31G**) for the analogous addition of triplet nitrene to ethylene.[27]

Conclusion

The calculations suggest that the rapid cycloaddition of a triplet methylene to a neighboring p bond results from the presence of the half-occupied in-plane σ orbital, which directly attacks the p system and also makes rotation out-of-plane much easier than for a singlet arylcarbene. More extensive comparison of rotational barriers in aromatic reactive intermediates will be reported in due course.[28]

Acknowledgment. We are grateful to the National Science Foundation for financial support of this research and to the Alexander von Humboldt Foundation for a U.S. Senior Scientist Award to K.N.H.

Registry No. (*E*)-**1a**, 117607-41-7; (*Z*)-**1a**, 117607-42-8; (*E*)-**1b**, 74346-41-1; (*Z*)-**1b**, 117607-43-9; **3a** (isomer 1), 117607-53-1; **3a** (isomer 2), 117677-91-5; (*E*)-**4a**, 117607-48-4; (*Z*)-**4a**, 117607-49-5; (*E*)-**4b**, 117607-50-8; (*Z*)-**4b**, 117607-51-9; (*E*)-**5a**, 117607-44-0; (*Z*)-**5a**, 117607-45-1; (*E*)-**5b**, 117607-46-2; (*Z*)-**5b**, 117607-47-3; *exo*-**6a**, 117607-52-0; *endo*-**6a**, 117706-80-6; *exo*-**6b**, 63949-51-9; *endo*-**6b**, 30021-35-3; phenylcarbene, 3101-08-4; methylene, 2465-56-7; ethene, 74-85-1.

---

(24) No ab initio computational study of the addition of triplet methylene to ethylene has been reported in the literature. Dewar and co-workers[25] used the semiempirical MINDO/2 procedure with an extension of the "half-electron" method[26] for calculations of triplet states. These calculations suggest that the initial approach of methylene to the alkene takes place symmetrically and that the carbene subsequently veers to one side of the double bond and attacks one of the ethylene carbon atoms to form the diradical. In the transition state, the carbon atom of the methylene moiety is at a distance of 2.1 Å from the closer ethylene carbon and 2.3 Å away from the farther one.

(25) Bodor, N.; Dewar, M. J. S.; Wasson, J. S. *J. Am. Chem. Soc.* **1972**, *94*, 9095.

(26) Dewar, M. J. S.; Hashmall, J. A.; Venier, C. G. *J. Am. Chem. Soc.* **1968**, *90*, 1953; Dewar, M. J. S.; Trinajstic, N. *J. Chem. Soc. D* **1970**, 646.

(27) Fueno, T.; Bonacic-Koutecky, V.; Koutecky, J. *J. Am. Chem. Soc.* **1983**, *105*, 5547.

(28) Dorigo, A.; Houk, K. N., submitted for publication.

Electrolytes in Charged Micropores

V. Vlachy[†] and A. D. J. Haymet*[‡]

Contribution from the Department of Chemistry, E. Kardelj University, Ljubljana 61000, Yugoslavia, and Department of Chemistry, University of California, Berkeley, California 94720. *Received June 6, 1988*

Abstract: We have studied a simple electrolyte enclosed within a charged cylindrical capillary and in thermodynamic equilibrium with an external solution, using the grand canonical Monte Carlo technique. Ionic correlation functions and mean activity coefficients have been evaluated at several charge densities and concentrations, and for several choices of capillary radius. Comparison with the results of the Poisson–Boltzmann equation is presented for all these quantities. The latter approximation is, as noticed previously, reasonably accurate if 1:1 electrolyte is present in a capillary. Important qualitative and quantitative differences are noticed for 2:2 simple electrolyte, even for moderate surface charge densities. Due to the interionic correlations, there is much more simple electrolyte present in the capillary than predicted by the mean-field theory. This affects the distribution of counterions and especially the mean activity coefficient of the electrolyte. Our simulations show that, at low charge densities, the mean activity coefficient of the electrolyte decreases with decreasing radius of the pore, while the Poisson–Boltzmann equation predicts the opposite behavior.

1. Introduction

The problem of adsorption of solute in liquid-filled pores has a number of important applications and is now being investigated intensively.[1,2] In this work, the structural and thermodynamic properties of ionic solution enclosed within the charged micropores are studied by two different theoretical methods. A number of electrochemical systems can be modeled as a cylindrical capillary with a charge distributed on the inner surface, immersed in an electrolyte solution. This model has been used to explain electrokinetic phenomena,[3-11] to describe ion selectivity in certain types of ion-exchange resins,[12] and to evaluate the activity of electrolyte within a capillary,[13-17] which may be useful in engineering applications. In all these studies (except ref 16) the Poisson–Boltzmann equation (sometimes in a linearized form) has been

---

[†] E. Kardelj University.

[‡] University of California.

(1) Nicholson, D.; Parsonage, N. G. *Computer Simulation and the Statistical Mechanics of Adsorption*; Academic Press: New York, 1982.

(2) Faraday Symposium No. 20 *J. Chem. Soc., Faraday Trans. 2* **1986**, *82*, 1569.

(3) Oldham, I. B.; Young, F. J.; Osterle, J. F. *J. Colloid Sci.* **1963**, *18*, 328.

(4) Dressner, L. *J. Phys. Chem.* **1963**, *67*, 1635.

(5) Rice, C. L.; Whitehead, R. *J. Phys. Chem.* **1965**, *69*, 4017.

(6) Morrison, F. A.; Osterle, J. F. *J. Chem. Phys.* **1965**, *43*, 2111.

(7) Jacazio, G.; Probstein, R. F.; Sonin, A. A.; Yung, D. *J. Phys. Chem.* **1972**, *76*, 4015.

(8) Levine, S.; Mariott, J. R.; Neale, G.; Epstein, N. *J. Colloid Interface Sci.* **1975**, *52*, 136.

(9) Olivares, W.; Croxton, T.; McQuarrie, D. A. *J. Phys. Chem.* **1980**, *84*, 867.

(10) Olivares, W.; McQuarrie, D. A. *J. Phys. Chem.* **1985**, *89*, 2966.

employed to calculate the mean electrostatic potential and the ionic distributions inside the capillary.

The validity of the Poisson–Boltzmann approximation has been the subject of several studies. In this context, the Monte Carlo simulations of planar[18-21] and cylindrical double layers,[22-26] which may serve as models for membranes, electrodes, or polyelectrolyte solutions, are valuable. The computer calculations indicate that the Poisson–Boltzmann equation describes adequately a 1:1 electrolyte in contact with a charged surface, but it fails to predict the correct behavior when divalent counterions are present in the solution. One such example is given in our previous study,[25] which models a DNA solution in the presence of 2:2 electrolyte. Though a similar conclusion about the validity of the Poisson–Boltzmann equation may be anticipated for the electrolyte in charged capillaries, there are some differences between this and the planar system, which has been the most thoroughly studied to date. The most important difference is that one deals not with a single (isolated) electrical double layer, but rather with an electrical double layer that extends throughout a capillary, similar to the system treated in ref 20. In other words, the local ionic concentrations inside the pore may differ everywhere and substantially from the bulk values at a given, fixed chemical potential. The radius of a capillary is therefore an additional and important parameter of the model.

In our previous work[16] an approximate integral equation, known in the literature as the HNC/MSA equation,[27] had been used to obtain the ionic correlation functions and the mean activity coefficient of the electrolyte inside the cylindrical pore. In this integral equation, which yields a rather accurate description of the interactions in the electrical double layer,[25,28] the corrections to the Poisson–Boltzmann equation are evaluated within the mean-spherical approximation.[29] The results of ref 16 give some additional evidence for the important role of the interionic correlations in solutions of divalent ions. These interionic correlations are ignored by the Poisson–Boltzmann approximation.

In order to measure accurately the ion–ion correlations and to evaluate the concentration of electrolyte enclosed within a cylindrical capillary, we have used the grand canonical Monte Carlo technique. The chemical potential of the solution inside is fixed by the external reservoir of electrolyte with concentration c_s at temperature T and chemical potential μ. This is a correct way to treat a system where no bulk phase is present explicitly.[18] The behavior of both 1:1 and 2:2 electrolytes is examined in this calculation. The charge density of the inner surfaces, concentration of the external (bulk) electrolyte c_s, and radius of the capillary are parameters of the model.

The outline of this paper is as follows. In section 2, the model and the principles of the Poisson–Boltzmann equation and the Monte Carlo method are presented. Our numerical results are collected in the third section. The local concentrations of the ions are shown as a function of the position within the pore. From the average concentration of co-ions, $\langle c_- \rangle$, and counterions, $\langle c_+ \rangle$, inside the cavity we can evaluate the exclusion parameter, or the mean activity coefficient of enclosed electrolyte. Of special interest are the variations of these quantities with the charge density and radius of the capillary. In both cases, our comparison indicates a breakdown of the Poisson–Boltzmann mean-field theory when 2:2 electrolyte is present in the capillary. The predictions of the Poisson–Boltzmann equation are not only quantitatively but also qualitatively incorrect, as discussed below in section 4.

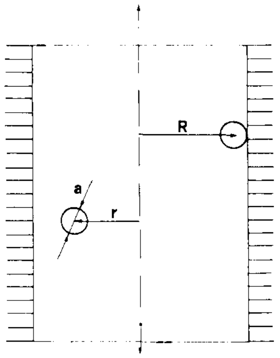

Figure 1. Cross section through the model capillary.

2. Micropore Model and Methods

The model used here is identical with that used in several previous articles,[3-17] and it is shown in Figure 1. We choose the inner surface of the cylindrical capillary to be negatively charged with a charge density

$$\sigma = ze_0/2\pi(R + a/2)h \tag{1}$$

where z is the number of elementary charges on the surface per length h and R is the radius of the cylinder within which the centers of the ions are distributed. The ions are charged hard spheres with a diameter a, so they can approach to the surface up to a distance $a/2$. The solvent is not included explicitly: it is viewed as a dielectric continuum of permitivity $\epsilon_0\epsilon_r$. The Poisson–Boltzmann equation for this system reads

$$\frac{1}{r}\frac{\mathrm{d}}{\mathrm{d}r}\left[r\frac{\mathrm{d}\psi}{\mathrm{d}r}\right] = -\frac{\rho_e}{\epsilon_0\epsilon_r} \tag{2}$$

$$\rho_e = z_+e_0n_+(0)\exp(-z_+e_0\psi\beta) + z_-e_0n_-(0)\exp(-z_-e_0\psi\beta) \tag{3}$$

where $\psi(r)$ is the mean electrostatic potential at a distance r, z_ie_0 is the charge of the ion i, and $n_i(0)$ its number concentration at the position $r = 0$, where ψ is chosen to be zero. This choice is only a matter of convenience, and if needed, the potential difference between the position $r = 0$ and the external solution can be evaluated.[16] As usual, $\beta^{-1} = k_BT$, where k_B is the Boltzmann constant and T is the absolute temperature. The solution of this differential equation can be obtained numerically subject to the boundary conditions given by eq 4 and 5. Here, as before,

$$\left.\frac{d\psi}{\mathrm{d}r}\right|_{r=0} = 0 \tag{4}$$

$$\left.\frac{\partial\psi}{\partial r}\right|_{r=R} = -\sigma/\epsilon_0\epsilon_r \tag{5}$$

an iterative numerical technique, also called the "shooting method", has been applied to solve eq 2–5.[30] The number densities $n_+(0)$ and $n_-(0)$ are related to the concentration of the bulk electrolyte n_s ($c_s = n_s/N_A$, where N_A is Avogadro's number) by the equation $n_s^2 = n_+(0)n_-(0)$.

The Poisson–Boltzmann approximation treats the ions as pointlike charges; it therefore ignores their size and, more importantly, their mutual correlations. Computer simulations are free of these approximations, and if the problems of finite size of the system can be addressed properly, they provide essentially exact results for a given model. The grand canonical Monte Carlo method has proved to be very useful in studies of the electrical double layer. The main advantage is that by sampling at constant chemical potential, rather than concentration, the relevant bulk electrolyte phase is defined unambiguously.[18,19,25] This is crucial in

---

(11) Christoforou, C. C.; Westermann-Clark, G. B.; Anderson, J. L. *J. Colloid Interface Sci.* **1985**, *106*, 1.

(12) Dolar, D.; Vlachy, V. *Vestn. Slov. Kem. Drus.* **1981**, *28*, 327.

(13) Dressner, L.; Krauss, K. A. *J. Phys. Chem.* **1963**, *67*, 990.

(14) MacGillivray, A. D.; Swift, J. D. *J. Phys. Chem.* **1968**, *72*, 3573.

(15) Dressner, L. *J. Phys. Chem.* **1963**, *67*, 2333.

(16) Vlachy, V.; McQuarrie, D. A. *J. Phys. Chem.* **1986**, *90*, 3248.

(17) Huertha, M.; Olivares, W. *J. Phys. Chem.* **1987**, *91*, 2975.

(18) Torrie, G. M.; Valleau, J. P. *J. Chem. Phys.* **1980**, *73*, 5807.

(19) Torrie, G. M.; Valleau, J. P. *J. Phys. Chem.* **1982**, *86*, 3251. Torrie, G. M.; Valleau, J. P.; Patey, G. N. *Ibid.* **1982**, *76*, 4615.

(20) Jönsson, B.; Wennerstrom, H.; Halle, B. *J. Phys. Chem.* **1980**, *84*, 2179.

(21) van Megen, W.; Snook, I. *J. Chem. Phys.* **1980**, *73*, 4556.

(22) Bratko, D.; Vlachy, V. *Chem. Phys. Lett.* **1982**, *90*, 434; *Ibid.* **1985**, *115*, 294.

(23) Le Bret, M.; Zimm, B. H. *Biopolymers* **1984**, *23*, 271.

(24) Murthy, C. S.; Bacquet, R. J.; Rossky, P. J. *J. Phys. Chem.* **1985**, *89*, 701.

(25) Vlachy, V.; Haymet, A. D. J. *J. Chem. Phys.* **1986**, *84*, 5874.

(26) Mills, P.; Anderson, C. F.; Record, M. T. *J. Phys. Chem.* **1986**, *89*, 6541.

(27) Gonzales-Tovar, E.; Lozada-Cassou, M.; Henderson, D. *J. Chem. Phys.* **1985**, *83*, 361.

(28) Vlachy, V.; McQuarrie, D. A. *J. Chem. Phys.* **1985**, *83*, 1927.

(29) Waisman, E.; Lebowitz, J. L. *J. Chem. Phys.* **1972**, *56*, 3086.

(30) Carnahan, B.; Luther, H. A.; Wilkes, J. O. *Applied Numerical Methods*; Wiley: New York, 1969.

Table I. Results of the Canonical Monte Carlo Calculations, for 1:1 and 2:2 Electrolyte at a Variety of Concentrations of the External Electrolyte c_s

run	$\sigma/(\mathrm{Asm}^{-2})$	R/nm	$\langle N_- \rangle$	c_s'	$c_s/[\langle c_+ \rangle \langle c_- \rangle]^{1/2}$
		1:1 Electrolyte[a]			
1	0.07111	4.0	39.41	0.0424	0.734 ± 0.01
2	0.1067	4.0	41.40	0.0381	0.647 ± 0.01
3	0.1422	4.0	30.26	0.0354	0.588 ± 0.01
		2:2 Electrolyte[b]			
4	0.03556	4.0	35.27	0.0386	0.705 ± 0.02
5	0.07112	4.0	37.12	0.0402	0.530 ± 0.01
6	0.1422	4.0	38.33	0.0433	0.376 ± 0.01
7	0.03556	2.0	31.15	0.0316	0.592 ± 0.01
8	0.03556	1.275	30.84	0.0256	0.525 ± 0.01
9	0.03556	0.85	28.2	0.0191	0.49 ± 0.01
		2:2 Electrolyte[c]			
10	0.03556	1.275	31.2	0.052	0.87 ± 0.01
11	0.03556	0.85	34.5	0.0402	0.80 ± 0.01

[a] $c_s = 0.1002$ mol dm^{-3}, $\gamma_{\pm,s} = 0.917$ (from ref 38). [b] $c_s = 0.0515$ mol dm^{-3}, $\gamma_{\pm,s} = 0.230$ (from ref 38). [c] $c_s = 0.1240$ mol dm^{-3}, $\gamma_{\pm,s} = 0.137$.

our study, since the electrical double layer extends throughout the capillary. An extensive description of the method is given in ref 18 and will only be summarized briefly here. The simulation procedure consists of two steps. The first step is canonical, and a randomly chosen ion is moved into a new random position somewhere in the cavity. The new position is accepted with the probability f_{ij},

$$f_{ij} = \min \{1, Y \exp[-(U_j - U_i)]\} \tag{6}$$

where U_i is the configurational energy of the state i, and $Y = 1$. The second step consists of either an attempted deletion of a neutral pair of randomly chosen ions or the attempted insertion of particles in some random positions. The transition probability from the state i with a number of co-ions N_i^- (N_i^+) to the state j where $N_j^- = N_i^- + 1$ (and $N_j^+ = N_i^+ + 1$) is given by combination of equations 6 and 7. In eq 7, $\gamma_{\pm,s}$

$$Y = \gamma_{\pm,s}{}^2 \frac{N_+ N_-}{N_j^+ N_j^-} \tag{7}$$

is the mean activity coefficient of the bulk electrolyte, where $N_+ = N_-$ and the concentration $c_s = N_-/(N_A \pi R^2 h)$.

In computer simulations of the anisotropic systems, the interactions of each particle with the part of the system outside the central cell must be included in the calculation in order to obtain the results for an effectively infinite thermodynamic system. One method has been suggested in previous simulations,[18] explicitly for a system similar to ours, by Rossky and co-workers.[24] With this method, the interaction outside the central cell is treated in the "mean-field" way, using the local concentrations of particles averaged over all previous configurations in the central cell to evaluate the corrections to the energies U_i and U_j. The average number of particles and other control parameters of the simulations are displayed in Table I.

3. Results

All results in this section are for water solutions at $T = 298$ K, where the relative permittivity of the system is $\epsilon_0\epsilon_r = 78.33$. The distance of closest approach "a" is chosen to be 0.425 nm to match that used in earlier computations. In Table I, the Monte Carlo results for the electrolyte concentration inside the cavity, $c_s' = \langle c_- \rangle$, are displayed for at several surface charge densities σ and for various choices of the radius of capillary. Before discussing the thermodynamic properties, it is interesting to see the spatial distribution of co-ions and counterions inside the capillary. These are given in Figures 2 and 3. Figure 2 shows clearly that the results of the Poisson–Boltzmann and Monte Carlo calculations for 1:1 electrolyte (run 1) are in good agreement for this range of concentrations and charge densities, as observed before.[18,25]

For divalent ions, the situation is quite different, as shown in Figure 3. Here the Poisson–Boltzmann approximation underestimates the ionic concentrations next to the charged surface. Strong correlations between the first layer of counterions and the co-ions make the concentration of the co-ions in the cavity considerably higher than predicted by the mean-field theory. To a certain degree, this is expected from previous simulations,[25] but the effect here has more dramatic consequences for the exclusion coefficient and for the mean activity coefficient of the enclosed electrolyte.

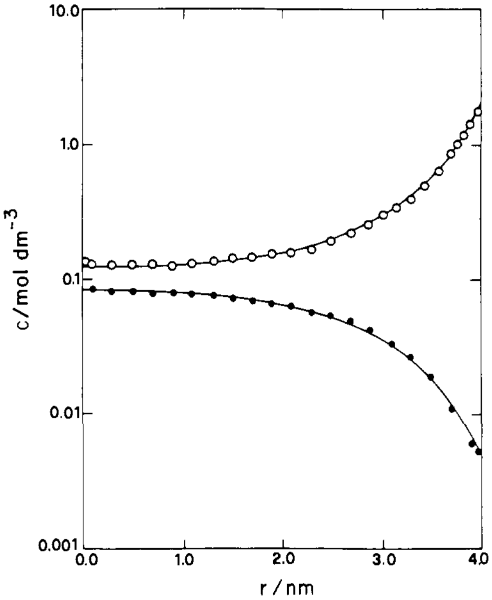

Figure 2. Local concentrations of co-ions (solid circles) and counterions (open circles) for 1:1 electrolyte inside the capillary, obtained from a Monte Carlo simulation and from the Poisson–Boltzmann equation (solid lines). The data is for run 1.

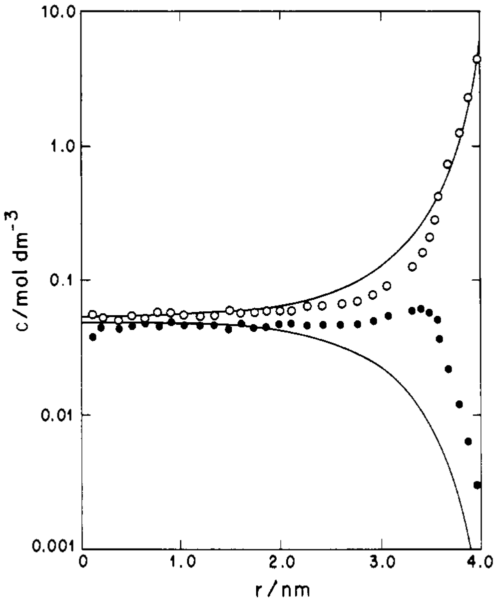

Figure 3. Same as Figure 2, but for 2:2 electrolyte inside the capillary. The data for run 6.

The equilibrium distribution of ions between a cavity and an external solution is determined by the condition that the total chemical potentials on both sides are equal.[31,32] In general, the pressure on one side may be different from that on the other and a potential difference between two solutions is present. The thermodynamic derivation for the mean activity coefficient in such systems is given in ref 32. Very frequently, it is a good approximation to assume that the activity of water does not differ appreciably between two solutions. In that case, a simplified equation applies:[32]

$$\gamma_\pm/\gamma_{\pm,s} = c_s/[\langle c_+ \rangle \langle c_- \rangle]^{1/2} \tag{8}$$

---

(31) Donnan, F. *Z. Electrochem.* **1911**, *17*, 572.

(32) Guggenheim, E. A.; *Thermodynamics* North Holland: Amsterdam, Holland, 1950.

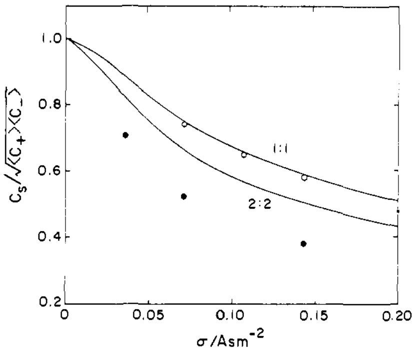

Figure 4. Ratio of the mean activity coefficients for 1:1 and 2:2 electrolyte as defined by eq 8. The solid lines are the Poisson–Boltzmann results, the circles are the grand canonical Monte Carlo data.

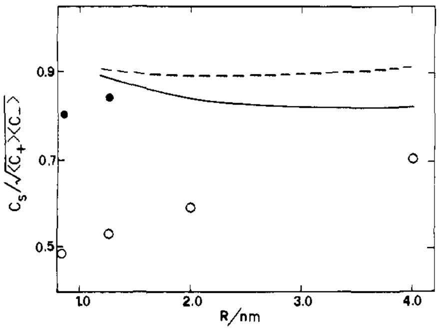

Figure 5. The ratio of the mean activity coefficient defined by eq 8 as a function of radius R. Open circles are the Monte Carlo results for $c_s = 0.0515$ mol dm^{-3} and filled circles for $c_s = 0.124$ mol dm^{-3}. The solid line is the prediction of the Poisson–Boltzmann theory for $c_s = 0.0515$ mol dm^{-3} and the dashed line for $c_s = 0.124$ mol dm^{-3}.

where $\gamma_\pm$ is the mean activity coefficient of the electrolyte enclosed in a cavity and $\gamma_{\pm,s}$, again, is the mean activity coefficient of the external (bulk) solution. This expression is exact if the net osmotic pressure in the system is zero. In this work the ratio of the activity coefficients $\gamma_\pm/\gamma_{\pm,s}$ as given by eq 8 is evaluated and presented in Figures 4 and 5.

Equation 8, with $\gamma_{\pm,s} = 1$, has also been derived by using the Poisson–Boltzmann equation[33] to describe the mean activity coefficient of the electrolyte in polyelectrolyte–electrolyte mixtures. Later, a more general derivation based on the density functional theory was presented.[28] Recently, another expression for the $\gamma_\pm$, valid within the framework of the Poisson–Boltzmann equation, has been proposed.[17] The new equation seems to yield numerical results different from those of 8. The ratio given by the r.h.s. of eq 8 ($\gamma_\pm/\gamma_{\pm,s}$) is presented in Figure 4 as a function of the surface charge density σ. As expected from the previous consideration of Figure 2, there is good agreement between the two different methods for 1:1 electrolyte. In contrast, the methods sharply disagree in the evaluation of the same quantity for 2:2 electrolyte in the capillary. The $c_s/[\langle c_+\rangle\langle c_-\rangle]^{1/2}$ ratio, evaluate by the Monte Carlo method, is considerably lower than predicted by the Poisson–Boltzmann equation even at the moderate charge densities.

Another way to present these results is to evaluate the exclusion coefficient, here defined as

$$\Gamma = (c_s - c_s')/c_s \tag{9}$$

Due to the negatively charged walls of the cavity, one would expect some of the negative ions to be expelled out of the capillary; that is, the inside concentration $\langle c_-\rangle = c_s'$ should be smaller than the bulk c_s. This is analogous to the Donnan effect in colloidal or polyelectrolyte solutions.[31-33] The results for c_s' given in Table I corroborate these expectations. The Monte Carlo coefficient, eq 9, is, however, much smaller than that obtained from the Poisson–Boltzmann approximation. Due to the intense interionic correlations between divalent ions, discussed already with respect to Figure 3, there is always more electrolyte present in the cavity than one would expect on the basis of the popular mean-field theory, i.e., the Poisson–Boltzmann equation.

More results demonstrating the breakdown of the conventional Poisson–Boltzmann theory for 2:2 electrolyte are presented in Figure 5. The ratio that approximates $\gamma_\pm/\gamma_{\pm,s}$ is here given as a function of the parameter R, where $R + a/2$ is the radius of the cylindrical capillary. The solid line represents the Poisson–Boltzmann results and circles are again the grand canonical Monte Carlo data. As is shown in Figure 5, the values of the $c_s/[\langle c_+\rangle\langle c_-\rangle]^{1/2}$ evaluated by the computer experiment get smaller for this choice of geometry, while the Poisson–Boltzmann results increase, with decreasing radius of the capillary. Since in the Poisson–Boltzmann model ions have zero diameters, the two sets of data are not strictly comparable. In any case, as a result of the mean-field approximation, too many ions are squeezed out of the capillary. At higher concentrations, higher surface charge densities, or for thinner pores, a complicated interplay of the excluded volume and electrostatic effects may take place. The Monte Carlo results for higher electrolyte concentrations (runs 10 and 11) are presented in Figure 5 as filled circles and the predictions of the Poisson–Boltzmann theory as a broken line.

We note that these simulations are relatively demanding in terms of computer time. A large number of particles (more than 1000) are needed to have at least 30 co-ions in the capillary and to obtain meaningful statistics. For example, a fully equilibrated run may require 5–6 h of CPU time on the CRAY X-MP/14 computer. This fact prevents immediate extension of our calculation to investigate the very interesting region of small radius R. We intend to present results for both charged and uncharged microcapillaries with a radius R of only a few ionic diameters in a separate study.

4. Conclusions

Numerical results for 1:1 electrolyte enclosed in a cylindrical cavity and in thermodynamic equilibrium with an external electrolyte solution of the same chemical composition confirm that the Poisson–Boltzmann equation retains its utility for solutions with monovalent counterions and at moderate charge densities. For a typical ion-exchange resin of technological importance, the surface charge density σ may be around 0.5 C/m^2,[13] which is higher than studied in this work and the results of the mean-field approximation are expected to be even *less* reliable in this case. The simulation results for 2:2 electrolyte show important effects of the ion–ion correlations neglected by the Poisson–Boltzmann theory.[18-22] The results of the latter approximation are not only quantitatively but also qualitatively incorrect. This has important implications for further studies of the electrokinetic and other phenomena such as electrofiltration or ion exchange. One particularly interesting case is when mono- and divalent counterions compete to enter into the charged capillary.[12] In view of the strong correlations between ions, some of the conclusions deduced from the classical Poisson–Boltzmann theory may have to be modified. Given the time-consuming nature of the computer simulations, some of the very successful theories of the electrical double layer, such as the hyper-netted chain (HNC) approximation,[34,35] should be adapted for this problem. The results also show that the behavior of cylindrical systems in many aspects is parallel to that of the simpler planar electrical double layers.[18-21] A breakdown of the Poisson–Boltzmann equation is suggested also by a recent Brownian dynamic simulation of the electrolyte between two charged planar surfaces.[36]

Physical theories always combine simplifications of the model with the approximations that are of statistical-mechanical origin. Though the deviations from the mean-field theory observed above are probably important, they only represent a part of the story. The second part involves the physical model, which ignores the discrete nature of the surface charges, the granularity of the

---

(33) Marcus, R. A. *J. Chem. Phys.* **1955**, *23*, 1057.

(34) Kjellander, R.; Marcelja, S. *Chem. Phys. Lett.* **1987**, *142*, 485, and references therein.

(35) Carnie, S. L. *Mol. Phys.* **1985**, *54*, 509.

(36) Åkesson, T.; Jönsson, B. *J. Phys. Chem.* **1985**, *89*, 2401.

solvent, and the effects of the dielectric boundary.[19,34] In addition, an exact treatment of electrokinetic phenomena is very complicated, notwithstanding the Poisson–Boltzmann equation; some radical approximations about the conductivity of the electrolyte in the cavity are usually accepted.[11] In this context, a nonequilibrium molecular dynamics study[37,38] of such a system would be a real step forward toward a better understanding of these important phenomena.

Acknowledgment. The support of the U.S.–Yugoslav Joint Fund for Scientific and Technological Cooperation (Project No. 8717984) is acknowledged gratefully. We thank a reviewer for comments that clarified the meaning of eq 8.

---

(37) Bitsaris, I.; Magda, J. J.; Tirell, M.; Davis, H. T. *J. Chem. Phys.* **1987**, *87*, 1733.

(38) Valleau, J. P.; Cohen, L. K. *J. Chem. Phys.* **1980**, *72*, 5935.

Solution Deuterium NMR Quadrupolar Relaxation Study of Heme Mobility in Myoglobin

Robert D. Johnson,[1] Gerd N. La Mar,* Kevin M. Smith, Daniel W. Parish, and Kevin C. Langry

Contribution from the Department of Chemistry, University of California, Davis, California 95616. *Received November 9, 1987*

Abstract: NMR spectroscopy has been used to monitor the quadrupolar relaxation and motional dynamics of ^2H selectively incorporated into skeletal and side chain positions of the heme in sperm whale myoglobin. The hyperfine shifts of the heme resonances in paramagnetic states of myoglobin allow resolution of the signals of interest, and paramagnetic contributions to the observed line widths are shown to be insignificant. The ^2H line widths for the skeletal positions of deuterohemin-reconstituted myoglobin yield a correlation time identical with that of overall protein tumbling (9 ns at 30 °C) and hence reflect an immobile heme group. The ^2H NMR line widths of heme methyl groups exhibit motional narrowing indicative of very rapid internal rotation. Hence the methyl rotation is effectively decoupled from the overall protein tumbling, and the residual quadrupolar line width can be used directly to determine the protein tumbling rate. The ^2H NMR lines from heme vinyl groups were found narrower than those from the heme skeleton. However, the range of quadrupolar coupling constants for sp^2 hybridized C–^2H bonds does not permit an unequivocal interpretation in terms of mobility.

The importance of dynamics to protein function has been recognized for some time, and it is currently an area of considerable research interest.[2-4] Hemoproteins have received particular attention in this regard, as the X-ray structures of myoglobin[5] and hemoglobin[6] reveal the necessity of structural fluctuations to allow for ligand access to the heme active site. Energy calculations have shown that structure fluctuations in myoglobin make ligand access energetically realistic,[7] and molecular dynamics calculations of amino acid residue fluctuations in cytochrome *c* have shown good agreement with residue mobility results derived from the temperature dependence of X-ray thermal factors.[4,8] The degree of steric interaction with an amino acid side chain, and hence the rotational mobility, of one of the heme vinyl groups in hemoglobin has been implicated in the cooperativity effect in human hemoglobin.[9] Several experimental methods have been employed to probe the great range of motional states in proteins.[2-4,10,11] One of the more versatile methods is NMR spectroscopy, which allows the characterization of the motions of specific atomic sites over a wide range of time scales. Analysis of relaxation rates such as T_1 and T_2 and the nuclear Overhauser effect (NOE) will yield motional information over a large range of rates.[2,3,12,13]

Several NMR relaxation experiments have been carried out on myoglobin. Solution studies include ^{13}C NMR at natural abundance,[14-16] using isotopically enriched ^{13}C methionines,[17] ^2H NMR of ^2H-labeled modified myoglobin,[18] and proton NOEs.[19,20] Crystalline state NMR has been used with ^{13}C-labeled methionines and ^2H-labeled heme methyl and propionic acids.[21-23] While ^{13}C and ^1H NMR relaxation experiments have furnished valuable insights into the dynamics of myoglobin, analysis of these experiments is not simple; some problems are the inverse sixth power dependence that the T_1's have on the internuclear distance, whose values are not known with precision, and the possibility of multiple

---

* Author to whom correspondence should be addressed.

(1) Current address: IBM Almaden Research, 650 Harry Road, San Jose, CA 95120.

(2) Gurd, F. R. N.; Rothgeb, T. M. *Adv. Protein Chem.* **1979**, *3*, 73–155.

(3) Karplus, M.; McCammon, J. A. *CRC Crit. Rev. Biochem.* **1981**, *22*, 293–348.

(4) McCammon, J. A.; Karplus, M. *Acct. Chem. Res.* **1983**, *16*, 187–193.

(5) Takano, T. J. *Mol. Biol.* **1977**, *110*, 537–568; 569–584.

(6) Perutz, M. F.; Matthews, F. S. *J. Mol. Biol.* **1966**, *21*, 199–202.

(7) Case, D. A.; Karplus, M. *J. Mol. Biol.* **1979**, *132*, 343–368.

(8) Northrup, S. H.; Pear, M. R.; Morgan, J. D.; McCammon, J. A. *J. Mol. Biol.* **1981**, *153*, 1687–1699.

(9) Gelin, J.; Karplus, M. *Proc. Natl. Acad. Sci. U.S.A.* **1979**, *76*, 801–805. Gelin, B. R.; Lee, A. W.-M.; Karplus, M. *J. Mol. Biol.* **1983**, *171*, 489–559.

(10) Debrunner, P. G.; Frauenfelder, H. *Annu. Rev. Phys. Chem.* **1982**, *33*, 283–299.

(11) Woodward, C. K.; Hilton, B. D. *Annu. Rev. Biophys. Bioeng.* **1979**, *8*, 99–127.

(12) Wüthrich, K. *Nuclear Magnetic Resonance in Biological Research-Peptides and Proteins*; North Holland: Amsterdam, 1976.

(13) Campbell, I. D.; Dobson, C. M.; Williams, R. J. P. *Adv. Chem. Phys.* **1978**, *39*, 55–70.

(14) Wittebort, R. J.; Rothgeb, T. M.; Szabo, A.; Gurd, F. R. N. *Proc. Natl. Acad. Sci. U.S.A.* **1979**, *76*, 1059–1063.

(15) Wilbur, D. J.; Norton, A. O.; Clouse, R.; Addleman, A.; Allerhand, A. *J. Am. Chem. Soc.* **1976**, *98*, 8250–8254.

(16) Visscher, R. B.; Gurd, F. R. N. *J. Biol. Chem.* **1975**, *250*, 2238–2242.

(17) Jones, W. C.; Rothgeb, T. M.; Gurd, F. R. N. *J. Am. Chem. Soc.* **1975**, *97*, 3875–3877.

(18) Oster, O.; Neireiter, G. W.; Clouse, A. O.; Gurd, F. R. N. *J. Biol. Chem.* **1975**, *230*, 7990–7996.

(19) Ramaprasad, S.; Johnson, R. D.; La Mar, G. N. *J. Am. Chem. Soc.* **1984**, *106*, 3632–3635.

(20) Ramaprasad, S.; Johnson, R. D.; La Mar, G. N. *J. Am. Chem. Soc.* **1984**, *106*, 5330–5335.

(21) Keniry, M. A.; Rothgeb, R. M.; Smith, R. L.; Gutowsky H. S.; Oldfield. E. *Biochemistry* **1983**, *22*, 1917–1926.

0002-7863/89/1511-0481$01.50/0